Focus-Tunable Microlens Arrays Fabricated on Spherical Surfaces

Difeng Zhu, Xuefeng Zeng, Chenhui Li, and Hongrui Jiang, *Senior Member, IEEE*

***Abstract*—We present microlens arrays consisting of multiple focus-tunable microlenses omnidirectionally fabricated on spherical surfaces, to realize large field of view. Thin flexible polymer bridges connecting adjacent microlenses are designed to reduce the wrapping stress and deformation of the microlens array. Each microlens, formed via water–oil interface, is individually tuned by a thermo-responsive hydrogel actuator. The range of the focal length of each microlens in this array varied from millimeters to infinity. A prototype of optical imaging system based on such a microlens array on a spherical surface, including a charged-coupled device camera, a fiber bundle, and a 3-D rotational stage, is demonstrated as well. [2010-0273]**

***Index Terms*—Curvilinear surface, field of view (FOV), focus tunable, microlens array.**

I. Introduction

OPTICAL imaging and microscopy have drawn considerable attention in biomedical, industrial, and military fields in the past decade, as their applications intend to keep up with the trend of device miniaturization [1]–[5]. Microlenses have been extensively used recently in those systems, such as photolithography [6], medical imaging [1], and optical communications [7]. In particular, focus-tunable microlenses, which eliminate the need for mechanical optical alignment or scanning, are considered possessing great potential to extend the current capability and applications [8]–[10]. However, traditional microlenses and microlens arrays suffer narrow field of view (FOV), which largely limits their applications [11], [12]. Thus, it is desirable to make microlens arrays onto curvilinear surfaces, like compound eyes of insects, in order to achieve large FOV [11], [13]. Nevertheless, this curvilinear structure could be difficult to realize due to the intrinsically planar nature of established fabrication techniques [12]. Although there are nonplanar fabrication processes developed, they are generally very complicated [12], [14], [15]. Furthermore, increased complexity in fabrication due to nonplanar geometry would make it relatively hard to fabricate tunable-focus microlenses, which would significantly restrict the optical information acquired [5], [16].

To overcome these challenges, a liquid-based focus-tunable microlens array omnidirectionally fabricated on a hemispherical surface would realize both large FOV and high spatial resolution. Preliminary results on the microlens array have been reported in [5] and [16] by our group. Here, we present more detailed studies on the fabrication of microlens arrays on spherical surfaces. Each microlens in this microlens array can be tuned in focal length individually, resulting in high spatial resolution. The tuned focal lengths of the microlens array range from millimeters to infinity. Thermo-responsive hydrogel rings perform as actuators for tuning, which avoids the requirement of complicated actuation systems [2], [17]–[19]. The adjacent microlenses are connected through thin polymer bridge structures to reduce the stress generated by wrapping on the spherical surfaces and, thus, the deformation in the microlens array. The fabrication process is relatively simple.

An optical imaging system based on the focus-tunable microlens array on a spherical surface is also demonstrated. This system consists of a microlens array on a transparent hemispherical shell, a fiber bundle, positioned inside the hemispherical shell, to capture images gathered from each microlens, a charged-coupled device (CCD) camera, and a 3-D rotational stage that is responsible of controlling the position of the fiber bundle.

II. Principle and Structure

Fig. 1(a) shows the 3-D schematics of one liquid-base focus-tunable microlens in an array fabricated on a spherical surface. A cavity, formed by a polymer substrate, a polymer slip that defines the aperture, and a hydrogel ring are filled with water, which is covered by silicone oil to prevent evaporation [5], [16]. Since the refractive index of silicone oil (1.48) is higher than that of water (1.33), a curved oil–water interface would form a lens. Surfaces of the polymer aperture slip are naturally hydrophobic, and the sidewall of the aperture slip is treated to be hydrophilic [17], [18]. Thus, a water–oil meniscus, whose circumference is pinned by a hydrophobic–hydrophilic (H–H) boundary at the top edge of the aperture, can be formed. Thermo-responsive reversible N-isopropylacrylamide (NIPAAm) hydrogel serves as the actuator to tune the focal length of the microlens. As the temperature decreases (increases), the hydrogel swells (contracts), regulating the curvature of the water–oil meniscus.[4], [5]. The water–oil interface

Manuscript received September 15, 2010; revised December 14, 2010; accepted December 29, 2010. Date of publication February 4, 2011; date of current version April 1, 2011. This work was supported in part by a Defense Advanced Research Projects Agency Grant (HR0011-08-1-0048), in part by a National Science Foundation Grant (ECCS 0745000), in part by the Wisconsin Institutes for Discovery, and in part by the Wallace H. Coulter Foundation. Subject Editor O. Solgaard.

D. Zhu, X. Zeng, and C. Li are with the Department of Electrical and Computer Engineering, University of Wisconsin, Madison, WI 53706 USA (e-mail: dzhu4@wisc.edu; xzeng2@wisc.edu; cli26@wisc.edu).

H. Jiang is with the Department of Electrical and Computer Engineering, the Materials Science Program, the Department of Biomedical Engineering, and the Eye Research Institute, University of Wisconsin, Madison, WI 53706 USA (e-mail: hongrui@engr.wisc.edu).

Color versions of one or more of the figures in this paper are available online at http://ieeexplore.ieee.org.

Digital Object Identifier 10.1109/JMEMS.2011.2105858

1057-7157/$26.00 © 2011 IEEE

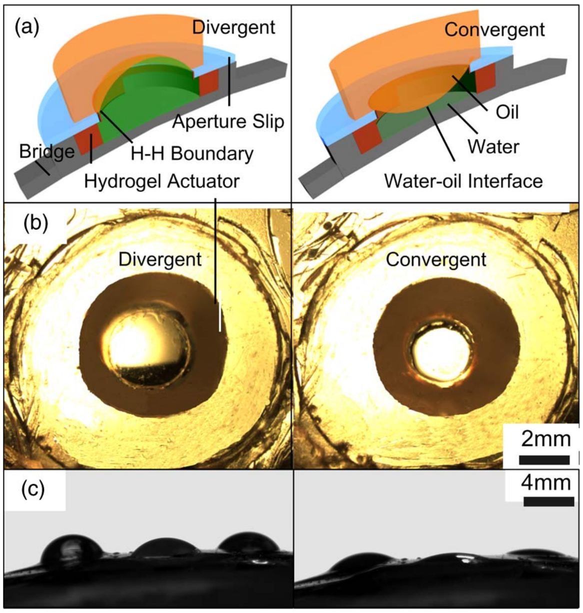

Fig. 1. (a) Schematics of one liquid-based focus-tunable microlens in divergent and convergent statuses, respectively. A water container is defined by a polymer slip, a hydrogel actuator, and the underlying polymer substrate. The sidewalls of the aperture are chemically treated to be hydrophilic by corona plasma discharge, while the top surfaces are naturally hydrophobic. An H–H boundary is generated to pin a meniscus, a curved interface between water and oil, which serves as a lens. The lens is divergent as the meniscus protrudes upward, while it turns convergent with the meniscus bulging downward. (b) Photoimages of a microlens in the two statuses: divergent and convergent. The (divergent) left image is taken at around 30 °C; the (convergent) right image is taken at about 50 °C. The scale bar is 2 mm. (c) Pictures of the side profiles of the water menisci of a three-element microlens array taken at different temperatures by a goniometer (without oil for visualization). Hydrogel actuators are below the lenses (not visible here). The left picture is taken at 30 °C, while the right one is taken at 45 °C. The scale bar is 4 mm.

protrudes upward at low temperatures (divergent) and bulges downward at high temperatures (convergent), as shown in Fig. 1(a). Therefore, the focal length of this liquid-base microlens is varied. Fig. 1(b) shows photoimages of a microlens in two statuses: divergent and convergent. Side profiles of the water menisci of the microlens structures on a curved surface can be observed via a goniometer (OCA 15+, DataPhysics Instruments, Inc., Germany), as shown in Fig. 1(c). Remarkable change in the radius of curvature of the water–air meniscus can be seen, corresponding to different temperatures. Note that the oil was not applied for visualization of the water menisci under the goniometer.

During the fabrication, the focus-tunable microlens array is first made planar. Then, to reach large FOV, the planar microlens array could be wrapped and fixed onto a curvilinear surface [5], [16]. As shown in Fig. 2(a), a six-element microlens array is wrapped onto a hemispherical acrylate shell with a diameter of 20 mm. When a planar substrate is wrapped onto a hemispherical surface, a resultant wrapping stress is generated, and the structure on the substrate would suffer severe deformation, degrading the optical performance of the microlens array. In order to reduce the wrapping stress and deformation, elastic polymer bridges [12] are used to connect each microlens structure, as indicated in the 3-D schematic in Fig. 2(b). The polymer bridges are around 200 μm in thickness, and the microlenses

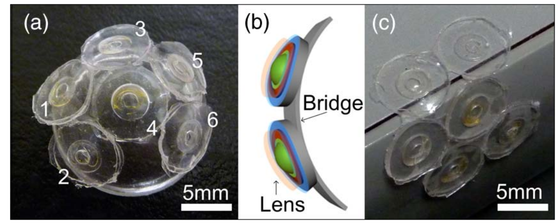

Fig. 2. (a) Six-element microlens array wrapped onto a hemispherical acrylate shell with a diameter of 20 mm. Each microlens element is connected with the adjacent one by elastic polymer bridges. Every lens is labeled with a number. The scale bar is 5 mm. (b) Schematic of the elastic polymer bridges, which connect adjacent microlens element. (c) Six-element microlens array folded at the edge of a desk.

structure is 450 μm thick. Owing to the difference in thickness, most wrapping stress is distributed in the polymer bridges, and thus, the deformation of the microlenses is reduced. Owing to the bridge structure, not only could this focus-tunable microlens array be wrapped onto a spherical surface with more ease, but it could also be bent or folded onto many other different kinds of nonplanar surfaces without noticeable deformation. Fig. 2(c) shows the six-element microlens array folded at the edge of a desk across two bridges. There is no visible damage to the microlenses even with such severe bending of the structure. Beyond its inherent planar nature, the capability of the microlens array is enhanced.

III. Fabrication

The fabrication process is based on a soft lithography process [20], [21] without clean room environment. In the whole procedure, four masked ultraviolet (UV) exposures are performed. The first two UV exposures define the geometry of the structure and the bridges of the microlens array, while the third UV exposure determines the geometry of the aperture slip. The liquid-base microlens array structure is realized by transferring from polymer molds. The last UV exposure is used to shape the thermal-responsive hydrogels as actuators.

A. *Equipment and Materials*

Photopolymerization procedures were carried out using a desktop EXFO Acticure 4000 (EXFO Photonic Solutions, Inc., Missisauge, ON, Canada) UV light source. Photomasks used were printed in high-resolution films (3000 dpi, Imagesetter, Inc., Madison, WI, USA). Oxygen plasma treatments were carried out using a corona plasma discharge.

There were three kinds of polymers used in this fabrication process: molds, structural polymer, and stimuli-responsive hydrogel. The detailed recipe can be found in previous publications [20]–[23]. The photopolymerizable prepolymer mixture solution [isobornylacrylate (IBA)] acts as molds. It is similar to negative photoresist. Exposure to a UV light source without air makes IBA crosslink and the prepolymer mixture solution solidify (called poly-IBA). Polydimethylsiloxane (PDMS), as the structural polymer, forms substrates, bridges, and apertures from the IBA molds. In our experiments, PDMS was cured from its original mixture state. The thermal-responsive hydrogel, serving as actuators, is responsible for the focus-tunable

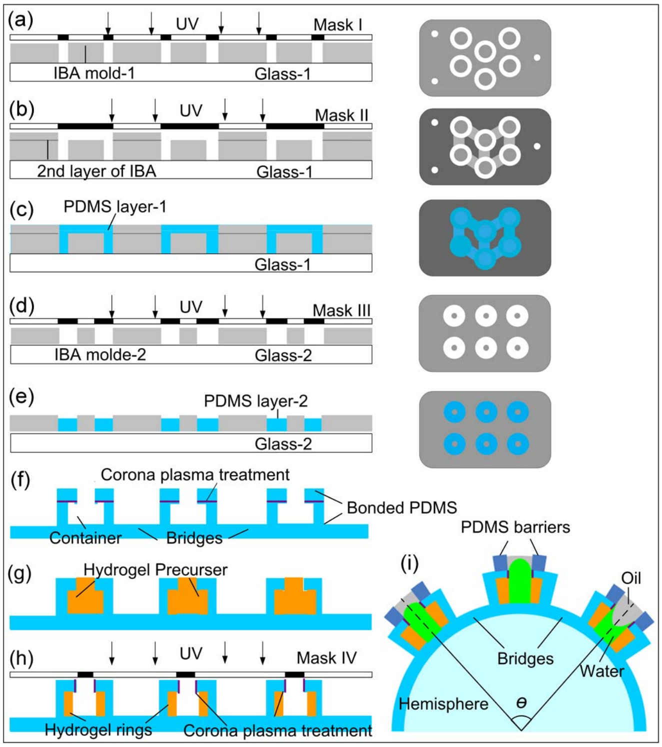

Fig. 3. Fabrication process flow of a six-element tunable-focus microlens array fabricated on a hemisphere. (a) IBA layer is initially photopatterned on a glass slide with Mask I. The right picture is the top view of the first layer of IBA mold. (b) Another IBA layer is photopatterned on the original IBA mold with Mask II. Mask II is aligned with the IBA substrate by three small circles on the edge, which could be seen from the top view on the right. By heightening certain part of the IBA layer in the second lithography, molds for bridge structure are realized. (c) PDMS mixture is poured onto the heightened IBA layer, serving as the substrate and bridges. Top view of the geometry of the PDMS is shown in the right picture. (d) Another IBA mold is photopatterned on the second glass slide with Mask III. (e) PDMS mixture is partially filled in the IBA mold, serving as the aperture layer of the microlens structure. (f) After being fully cured on hot plates, two PDMS layers are stripped from their molds. Corona plasma treatment is performed on their surfaces. The microlens cavities are formed by bonding together two PDMS layers treated to be hydrophilic. (g) NIPAAm precursor is injected into six cavities. (h) NIPAAm hydrogel rings are photopatterned in the cavities as actuators with Mask IV. The sidewall of the aperture slip is treated from hydrophobic to hydrophilic. (i) Water–oil interface is formed at the edge of each aperture slip due to the surface tension at the H–H boundary, serving as a lens. The microlens array is wrapped onto a hemispherical base and is distributed on a cap. θ is defined as the angle that this cap subtends. A separately fabricated round PDMS barrier (similar fabrication process but is not shown here) is placed onto each microlens to keep oil in the package.

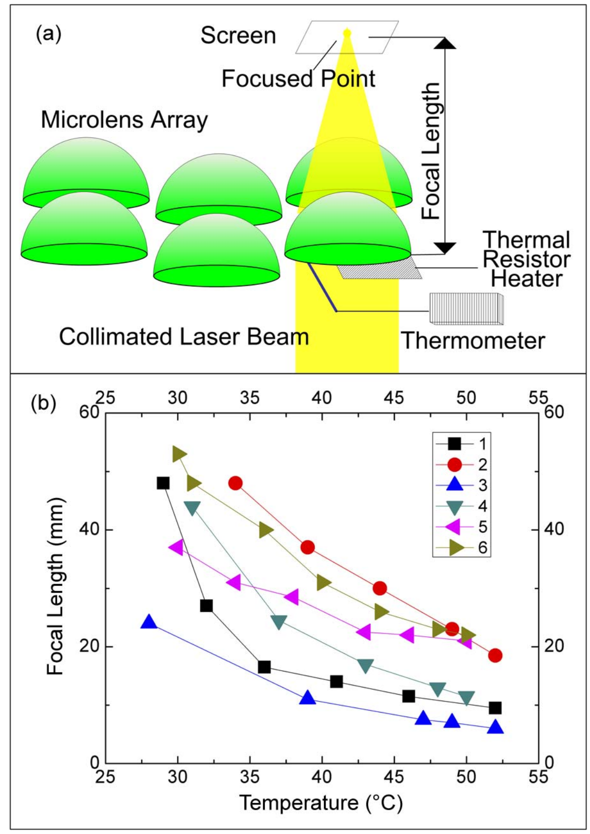

Fig. 4. (a) Schematic of testing the focal length tunability of each microlens in the six-element microlens array. Focal length of each microlens at different temperature is measured by determining the position of the optically minimum focused point of a collimated input light beam along the optical axis. A thermal resistor heater and a thermometer are positioned under the microlens in order to control and measure the *in situ* surrounding temperature, while the focused point of a microlens is recorded. (b) Dynamic change in the focal length of each microlens, labeled in Fig. 2(a), at different temperatures. The focal length ranges from several millimeters to infinity, as the temperature varies from 25 °C to 53 °C.

ability of each microlens. Here, thermal-responsive hydrogel N-isopropylacrylamide (NIPAAm) is utilized for thermal control of the focus-tunable microlens. It can be solidified under UV radiance, like negative photoresist. Ring-shaped NIPAAm hydrogel actuators were photopatterned under the aperture slip in our experiment, which would vary the pressure to the menisci, thus changing the curvature of the water–oil interfaces.

B. Fabrication Process

The fabrication process is illustrated in Fig. 3. First, IBA substrate mold was formed in a polycarbonate cartridge well (40 × 22 mm, HybriWells, Grace Bio-Labs, Inc., Bend, OR, USA). The cartridge well consists of top cartridge plates and bottom liner plates adhered together by a 250-μm-thick spacer (double-sided adhesive tape; 3M Corporate Headquarters, St. Paul, MN) at the edge. IBA-based prepolymer mixture solution was flowed into the well using transfer pipettes. The first film photomask (Mask I) was positioned on top of the cartridge plate and was exposed to UV light source (intensity, UV $= 9$ mW/cm^2; time, $t = 20$ s) to form the poly-IBA aperture array, as shown in Fig. 3(a) (top view on the right). The bottom liner plate was then peeled off. Unpolymerized prepolymer solution was rinsed away with ethanol. Then, another layer of IBA polymer was formed onto the patterned structures under UV radiance (intensity, $I = 9$ mW/cm^2 ; time, $t = 20$ s) with Mask II to increase the height of selected areas with the same methods, corresponding to the ultimate bridge structures, as shown in Fig. 3(b). A 200-μm-thick spacer was positioned between the top cartridge plate and the patterned IBA mold in order to determine the height of bridges. Mask II was aligned on the second cartridge with the patterned IBA mold utilizing three small circles at the edge, as shown in the right picture (top view) of Fig. 3(b). A similar procedure was executed on a glass slide to form another mold, whose height was around 120 μm, for the fabrication of the aperture slip, as shown in Fig. 3(d). Then, both IBA molds were transferred to PDMS to serve as the substrate and aperture slip, respectively, as shown in Fig. 3(c) and (e). The liquid level of the PDMS mixture was lower than the IBA mold to form through the holes as the apertures. PDMS mixture was then cured on a hot plate at 65 °C for 4 h. Next, two fully cured PDMS layers were peeled off from the respective molds.

After the inner surfaces of the cavities were treated from hydrophobic to hydrophilic by corona plasma discharge, two PDMS layers were bonded together [24], as shown in Fig. 3(f), to form the structure. Then, the bonded PDMS structure was pressed by 20-lb loads for two days, in order to prevent leakage between bonded layers.

Next, NIPAAm precursor was injected into the cavities, as shown in Fig. 3(g), and was photopatterned under UV light (intensity $I = 13.5$ mW/cm^2; time $t = 8.5$ s), with Mask IV aligned with the aperture slip. Noncrosslinked hydrogel precursor was flushed away by ethanol, and NIPAAm hydrogel rings were formed in the cavities. The sidewall of the aperture slip was treated by corona plasma discharge to be hydrophilic to pin the water–oil menisci, as shown in Fig. 3(h).

Then, this planar microlens array with soft PDMS substrate was wrapped onto a hemispherical base. Finally, each cavity was filled with water and covered by silicone oil, forming the water–oil interface, as shown in Fig. 3(i). Separately fabricated PDMS barriers were used to keep the oil in the package. The fabrication procedure of these PDMS barriers is not shown in the figure.

The diameter of each microlens was 1.8 mm. Each cavity was 250 μm in depth and 4 mm in diameter. The bridge was around 200 μm thick, 0.8 mm wide, and 0.8 mm long. The shape of the original water–oil interface was determined by the volume of water filled.

IV. Experiments and Results

A. Focal Length, Tunability, FOV, and Wrapping Stress Analysis

As shown in Fig. 4(a), the focal length of each microlens in the array was initially measured before wrapping on a hemispherical base, as a way of determining the position of the optically minimum focused point of a collimated input light beam along the optical axis [25]. A small thermal resistor heater and the tip of a thermometer were placed under the target microlens in order to control and measure the *in situ* surrounding temperature, while the focused point of a microlens was being recorded. The dynamic focal lengths of the six microlenses at different temperatures ranging from 53 °C to 25 °C were obtained, as plotted in Fig. 4(b). The positive focal lengths of the six microlenses varied from (1) 9.5, (2) 18, (3) 7, (4) 12.5, (5) 21.5, and 22 mm (6), respectively, to infinity. The number of each microlens was labeled in Fig. 2(a). Due to the nonuniformity in patterning the hydrogel actuators with our exposure system and various volume of water injected into the individual cavity, nonuniformity was manifested in Fig. 4(b). The average depth of focus was measured to be around 4.5 mm.

The tunable-focus microlens array would be wrapped on a hemispherical dome and a hemispherical shell with a diameter of 18 and 20 mm, respectively, for testing. The FOV analysis was first performed here. The FOV of each lens was measured

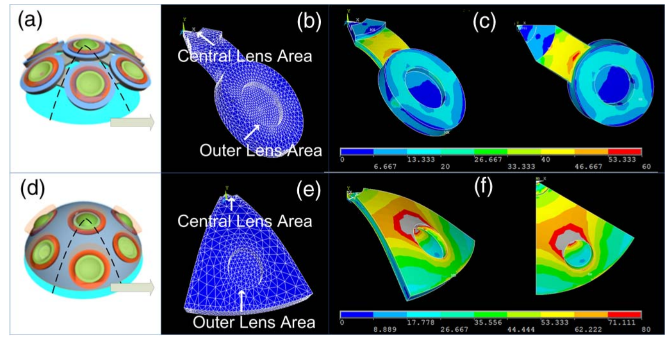

Fig. 5. (a) Microlens array with bridge structures and a hemispherical base. One-sixth of the structure is built in ANSYS as Model 1. Geometric parameters for Model 1: diameter and thickness of one chamber where water–oil interface resides: 1.5 and 0.25 mm; diameter and thickness of the complete circular polymer structure: 3 and 0.5 mm; bridges: 3 mm by 3 mm by 0.25 mm. (b) Meshed polymer structure of Model 1 after loads. (c) Deformed polymer structure and the stress distribution of Model 1. (d) Microlens array without bridge structure and a hemispherical base. One-sixth of the structure is built in ANSYS as Model 2. Geometric parameters for Model 2: diameter of the polymer structure without bridge: 12 mm; diameter and thickness of one chamber where microlens resides: 1.5 and 0.25 mm; thickness of the substrate under the microlens: 0.25 mm. (e) Meshed polymer structure of Model 2 after loads. (f) Deformed polymer structure and the stress distribution corresponding to the load for Model 2.

to be from 77° to 128°, depending on the focal length of the lens [26]. In the microlens array fabricated on the 18-mm-diameter dome, lenses were distributed on a spherical cap with an angle θ of about 116° [θ is defined in Fig. 3(i)]. For the microlens array distributed on the 20-mm-diameter shell, θ is 113°.

Quantitative stress analysis on how the bridge structure absorbs stress in the wrapping process was next performed using commercial software ANSYS (ANSYS 12.1 Release, ANSYS, Inc.). Due to axial symmetry, one sixth of the six-element microlens array on a hemispherical base was sampled in ANSYS for simplicity. Symmetric boundary conditions were applied to corresponding surfaces to improve the accuracy. The polymer structure with bridges was built in ANSYS as Model 1, while a polymer structure without bridges was also established as Model 2 to be a control, as shown in Fig. 5(a) and (d).

Parameters set for Model 1 were as follows: structural material (PDMS): Young's modulus of 750 kPa; Poisson's Ratio of 0.49; diameter and thickness of one complete circular polymer structure representing the fringe and the substrate of a microlens: 3 and 0.5 mm, respectively; diameter and thickness of a chamber where the microlens (water–oil interface) resides: 1.5 and 0.25 mm, respectively; and bridge structure: 3 mm by 3 mm by 0.25 mm. Multiple displacements were loaded on the polymer structure in order to make it bend as if it was contacted with a hemispherical base. The meshed structure after the loads of Model 1 is illustrated in Fig. 5(b), and the deformed structure and stress distribution is illustrated in Fig. 5(c). As can be seen, intense stress (over 30 kPa) is concentrated in the bridge area. The circular areas where the liquid microlenses reside only experience stress less than 15 kPa. Compared to the area with the bridges, the lens areas could be considered immune to the stress during the wrapping process. There would be little deformation at those areas based on the simulation.

In contrast, meshed structure of Model 2 of the polymer microlens array without bridges and deformed structure and the

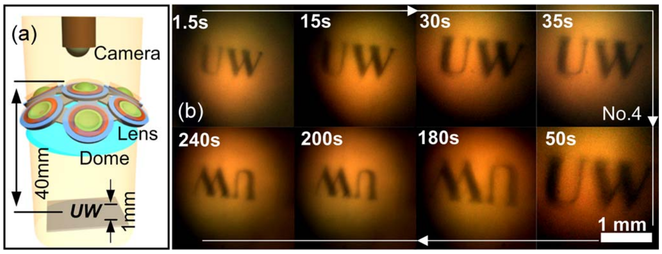

Fig. 6. (a) Three-dimensional schematics of testing the imaging of the microlens array on the glass hemisphere with a diameter of 18 mm. A transparency film with a logo of "UW" (1 mm in size) is placed 40 mm below the microlens array. A CCD-coupled stereoscope is responsible for recording images. (b) Frame sequence of the focused images from one typical microlens (number 4) in this microlens array in one scan. The microlens is initially convergent, and real images are obtained. Then, the focal length of the microlens gradually increases as the hydrogel actuator expands with thermal dissipation. As a result, the real images are magnified with time. Then, the microlens switches to the divergent status after around 80 s; thus, the images are inverted as virtual images after being refocused. As the temperature further cools down, the negative focal length keeps increasing, resulting in the increase in size of virtual images. The change in size of one microlens (number 4) is consistent with the dynamic change in focal length indicated in Fig. 4(b). The scale bar is 1 mm.

stress distribution after displacements are shown in Fig. 5(e) and (f), respectively. Corresponding parameters were as follows: structural material (PDMS) with Young's modulus of 750 kPa and a Poisson's ratio of 0.49, respectively; diameter and thickness of the polymer structure without bridge: 12 and 0.5 mm, respectively; and the diameter and thickness of the chamber where the microlens would reside: 1.5 and 0.25 mm, respectively. Similar boundary conditions and loads were exerted. Unlike disproportionate stress distribution in Model 1, as shown in Fig. 5(c), the stress in Model 2 is distributed relatively uniformly on the whole polymer structure. The stress near the outer lens area is far over 50 kPa and that near the central area is over 40 kPa, about five times of the stress in Model 1 at the similar position. Such stress would deform the water–oil interface and thus degrade the optical performance of the microlens.

By comparing the two cases, it can be concluded that the bridge structure could effectively reduce the wrapping stress, therefore minimizing the unwanted deformation of the liquid microlens structure.

The setup to test the imaging of the fabricated tunable-focus microlens array on a transparent dome with a diameter of 18 mm is shown in Fig. 6(a). An object plane with a logo of "UW" (1 mm in size) was positioned 40 mm below this microlens array (including the underlying hemispherical glass dome). A CCD-coupled stereoscope was positioned above this microlens array to monitor and capture images obtained from the microlenses. The microlens array wrapped on the dome was initially heated to 55 °C on a hot plate. Next, the microlens array was removed from the heat and placed under the stereoscope. As the device was cooled down to room temperature (23 °C) by thermal dissipation, images from the microlenses were recorded. The frame sequence from the recorded video of one typical microlens (number 4) is shown in Fig. 6(c). The magnification and inversion of the focused images are observed. Note that the hemispherical glass dome also contributes to the ultimate images.

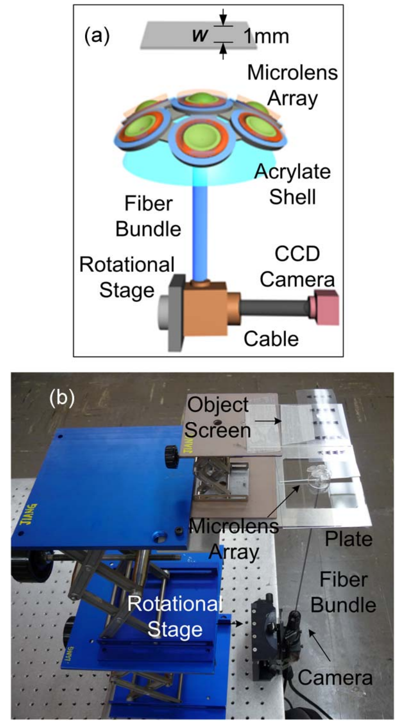

Fig. 7. (a) Schematic of a simple optical imaging system demonstrated based on the curvilinear focus-tunable microlens array. This system consists of a six-element microlens array on a hemispherical acrylate shell with a diameter of 20 mm, an optical fiber bundle, a rotational stage, and a CCD camera that connects with a PC. A transparency film with a logo "W" (1 mm in size) is placed around 20 mm above the microlens array. (b) Photo of this prototype system.

After the removal of the device from the hot plate, the microlens was initially convergent. Due to thermal dissipation, hydrogel actuators gradually expanded, bulging up the water–oil meniscus, thus flattened the interface. Therefore, the focal length increased from several millimeters to infinity, and as a result, the image was magnified in this process. With further decreasing temperature, the hydrogel kept swelling so that the water–oil interface bulged up. Thus, the microlens switched from convergent to divergent at around 80 s; the inverted virtual images were obtained at another point of the optical axis. As the temperature kept going down, the inverted images gradually shrunk, indicating an increase in the negative focal length. During the whole recording process, the stereoscope was fine tuned to keep the images clear.

B. Prototype of Optical Imaging System

The liquid-based focus-tunable microlens array could be integrated with many optical imaging systems. A prototype optical imaging system is demonstrated here, including the microlens array on a spherical surface, a fiber bundle (MilliscopeII, Zibra Corporation, Westport, MA, USA), rotational stage, and a CCD camera. Fig. 7(a) illustrates the schematic of this detection system. A six-element microlens array on an acrylate hemispherical shell with a diameter of 20 mm was positioned on a plate. An optical fiber bundle, connected with a CCD camera, was inserted into the shell so as to capture images obtained from each microlens. The fiber bundle was attached to a 3-D rotational stage. Owing to that,

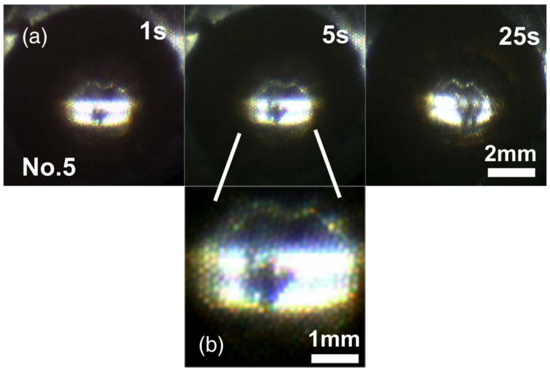

Fig. 8. (a) Frame sequence of the focused images captured by the simple optical system in Fig. 7. The images are obtained from one microlens (lens number 5: top of the shell) in this microlens array in one scan. Owing to thermal dissipation, the focal length of the microlens gradually increases, and thus, the real images are magnified with time. The scale bar is 2 mm. (b) Magnified photo of lens number 5 at 5 s. Pixels can be observed. The image quality is restricted by the relatively low resolution of the optical fiber bundle. The scale bar is 1 mm.

the fiber bundle could move forward or backward and rotate at a certain angle as well. As a result, it could receive optical information from different microlenses in the array and record images while the focal length of the target microlens is tuned. An object plane with a logo of "W" (1 mm in size) is positioned 20 mm above this microlens array. A photo of this prototype system is shown in Fig. 7(b).

The testing procedure was similar to focal length tunability test shown in Section IV-A. The microlens array wrapped on the shell was also initially heated to 55 °C and then cooled down to room temperature (23 °C) by thermal dissipation. As the temperature of hydrogel actuators gradually approaches room temperature, images obtained from the microlenses were transmitted through the fiber bundle and captured by the CCD camera. The typical frame sequence from the recorded images of one microlens (number 5) is shown in Fig. 8(a). Magnification of the focused images was observed as well, indicating the variance in focal length of the microlens. Note that the image quality is limited by the resolution of the optical fiber bundle. Pixelization of the image—each pixel corresponding to one fiber in the bundle can be observed in Fig. 8(b). Moreover, the fiber bundle is a commercial product fully packaged. In our experiments, when inserting the fiber bundle into the acrylate shell, we have limited capability to accurately adjust the position and angle of the fiber bundle. This also limited the image quality obtained.

V. Conclusion

In summary, we have demonstrated focus-tunable microlens arrays with six elements on spherical surfaces. Liquid-based microlenses were omnidirectionally fabricated on transparent hemispherical bases with diameters of 18 or 20 mm, respectively, in order to realize large FOV. The microlenses were distributed on a cap subtending an angle of 113° (20-mm-diameter base) or 116° (18-mm-diameter base). Thin flexible PDMS bridges connecting each adjacent microlens are designed to reduce the wrapping stress and deformation of the microlens array. Each microlens is individually tuned by a thermo-responsive hydrogel actuator fabricated around it. The range of the focal length of each microlens in this array varied from millimeters to infinity. A prototype of optical imaging system based on this focus-tunable microlens array has been demonstrated as well. A CCD camera, connected with a fiber bundle, which was inserted into the hemispherical shell, captured images obtained from each microlens. This system provides a prototype for many potential applications, such as endoscopes in medical imaging [1] and surveillance systems [27].

In future studies, the uniformity of the microlenses in the array would be improved through better lithography systems and precise control of the volume of the water filled into the cavity. A larger FOV is expected by covering a whole sphere with microlens arrays with more lens elements [28], and thus, a distributed angle approaching 360° could be realized. The microlens array will be developed on arbitrary curvilinear surfaces. Ray aberration of the curvilinear microlens would be characterized. Metal resistive microheaters and thermal coupling microsensors could be fabricated below each single hydrogel actuator to control the temperature locally. A thermal insulating layer would be utilized to reduce the crosstalk among the hydrogel actuators. The prototype of the optical system based on this microlens array will be further improved. Multiple wave guides could be introduced to transmit information obtained from different microlenses simultaneously [13]. Flexible optoelectronics could be integrated to widen its applications [12].

Acknowledgment

The authors would like to thank Dr. D. Cheng and Y. Liu for discussions and the Computer-Aided Engineering at the University of Wisconsin, Madison, for access to the software of ANSYS 12.1. This research utilized the National Science Foundation supported shared facilities at the University of Wisconsin, Madison.

References

[1] K. Carlson, M. Chidley, K. B. Sung, M. Descour, A. Gillenwater, M. Follen, and R. Richards-Kortum, "In vivo fiber-optic confocal reflectance microscope with an injection-molded plastic miniature objective lens," *Appl. Opt.*, vol. 44, no. 10, pp. 1792–1797, Apr. 2005.

[2] D. Zhang, V. Lien, Y. Berdichevsky, J. Choi, and Y.-H. Lo, "Fluidic adaptive lens with high focal length tunability," *Appl. Phys. Lett.*, vol. 82, no. 19, pp. 3171–3172, May 2003.

[3] H. Ren and S. T. Wu, "Variable-focus liquid lens by changing aperture," *Appl. Phys. Lett.*, vol. 86, no. 21, pp. 211107-1–211107-3, May 2005.

[4] C.-C. Cheng, C. A. Chang, C.-H. Liu, and J. A. Yeh, "A tunable liquid-crystal microlens with hybrid alignment," *J. Opt. A: Pure Appl. Opt.*, vol. 8, no. 7, pp. 365–369, Jul. 2006.

[5] D. Zhu, C. Li, X. Zeng, and H. Jiang, "Tunable-focus microlens arrays on curved surfaces," *Appl. Phys. Lett.*, vol. 96, no. 8, pp. 081111-1–081111-3, Feb. 2010.

[6] M. H. Wu and G. M. Whitesides, "Fabrication of diffractive and micro-optical elements using microlens projection lithography," *Adv. Mater.*, vol. 14, no. 20, pp. 1502–1506, Oct. 2002.

[7] H. Hamam, "A two-way optical interconnection network using a single mode fiber array," *Opt. Commun.*, vol. 150, no. 1–6, pp. 270–276, May 1998.

[8] N. Chronis, G. L. Liu, K. H. Jeong, and L. P. Lee, "Tunable liquid-filled microlens array integrated with microfluidic network," *Opt. Express*, vol. 11, no. 19, pp. 2370–2378, Sep. 2003.

[9] C.-C. Cheng, C. A. Chang, and J. A. Yeh, “Variable focus dielectric liquid droplet lens,” *Opt. Express*, vol. 14, no. 9, pp. 4101–4106, May 2006.
[10] H. Ren, Y. Lin, and S. T. Wu, “Adaptive lens using liquid crystal concentration redistribution,” *Appl. Phys. Lett.*, vol. 88, no. 19, pp. 191116-1–191116-3, May 2006.
[11] J. W. Duparre and F. C. Wippermann, “Micro-optical artificial compound eyes,” *Bioinspiration Biomimetics*, vol. 1, no. 1, pp. R1–R16, Mar. 2006.
[12] H. C. Ko, M. P. Stoykovich, J. Song, V. Malyarchuk, W. M. Choi, C.-J. Yu, J. B. Geddes, III, J. Xiao, S. Wang, Y. Huang, and J. A. Rogers, “A hemispherical electronic eye camera based on compressible silicon optoelectronics,” *Nature*, vol. 454, no. 7205, pp. 748–753, Aug. 2008.
[13] K.-H. Jeong, J. Kim, and L. P. Lee, “Biologically inspired artificial compound eyes,” *Science*, vol. 312, no. 5773, pp. 557–561, Apr. 28, 2006.
[14] D. Radtke, J. Duparré, U. D. Zeitner, and A. Tünnermann, “Laser lithographic fabrication and characterization of a spherical artificial compound eye,” *Opt. Express*, vol. 15, no. 6, pp. 3067–3077, Mar. 2007.
[15] R. J. Jackman, J. L. Wilbur, and G. M. Whitesides, “Fabrication of submicrometer features on curved substrates by microcontact printing,” *Science*, vol. 269, no. 5224, pp. 664–666, Aug. 1995.
[16] D. Zhu, C. Li, X. Zeng, and H. Jiang, “Hydrogel-actuated tunable-focus microlens arrays mimicking compound eyes,” in *Proc. 15th Int. Conf. Solid-State Sens., Actuators, Microsyst. (Transducers)*, Denver, CO, 2009, pp. 2302–2305.
[17] L. Dong, A. K. Agarwal, D. J. Beebe, and H. Jiang, “Adaptive liquid microlenses activated by stimuli-responsive hydrogels,” *Nature*, vol. 442, no. 7102, pp. 551–554, Aug. 2006.
[18] L. Dong, A. K. Agarwal, D. J. Beebe, and H. Jiang, “Variable-focus liquid microlenses and microlens arrays actuated by thermoresponsive hydrogels,” *Adv. Mater.*, vol. 19, no. 3, pp. 401–405, Feb. 2007.
[19] X. Zeng and H. Jiang, “Tunable liquid microlens actuated by infrared light responsive hydrogel,” *Appl. Phys. Lett.*, vol. 93, no. 15, pp. 151101-1–151101-3, Oct. 2008.
[20] A. K. Agarwal, D. J. Beebe, and H. Jiang, “Integration of polymer and metalmicrostructures using liquid-phase photopolymerization,” *J. Micromech. Microeng.*, vol. 16, no. 2, pp. 332–340, Feb. 2006.
[21] A. K. Agarwal, S. S. Sridharamurthy, D. J. Beebe, and H. Jiang, “Programmable autonomous micromixers and micropumps,” *J. Microelectromech. Syst.*, vol. 14, no. 6, pp. 1409–1421, Dec. 2005.
[22] Y. N. Xia and G. M. Whitesides, “Soft lithography,” *Annu. Rev. Mater.Sci.*, vol. 28, pp. 153–184, 1998.
[23] S. S. Sridharamurthy, A. K. Agarwal, D. J. Beebe, and H. Jiang, “Dissolvable membranes as sensing elements for microfluidics based biological/chemical sensors,” *Lab Chip*, vol. 6, no. 7, pp. 840–842, May 2006.
[24] K. Haubert, T. Drier, and D. Beebe, “PDMS bonding by means of a portable, low-cost corona system,” *Lab Chip*, vol. 6, no. 12, pp. 1548–1549, Dec. 2006.
[25] X. Zeng and H. Jiang, “An endoscope utilizing tunable-focus microlenses actuated through infrared-light,” in *Proc. 15th Int. Conf. Solid-State Sens., Actuators, Microsyst. (Transducers)*, Denver, CO, 2009, pp. 116–119.
[26] X. Zeng and H. Jiang, “Polydimethylsiloxane microlens arrays fabricated through liquid-phase photopolymerization and molding,” *J. Microelectromech. Syst.*, vol. 17, no. 5, pp. 1210–1217, Oct. 2008.
[27] X. Agarwal, R. A. Gunasekaran, P. Coane, and K. Varahramyan, “Polymer-based variable focal length microlens system,” *J. Micromech. Microeng.*, vol. 14, no. 12, pp. 1665–1673, Dec. 2004.
[28] X. Zeng, C. Smith, J. Gould, C. Heise, and H. Jiang, “Fiber endoscopes utilizing liquid tunable-focus microlenses actuated through infrared light,” *J. Microelectromech. Syst.*, in revision.

Difeng Zhu received the B.S. degree from the Department of Microelectronics, Peking University, Beijing, China, in 2007. He is currently working toward the Ph.D. degree in electrical engineering at the University of Wisconsin, Madison.

His research interests include the liquid focus-variable microlens, optical microelectromechanical systems, and flexible electronics.

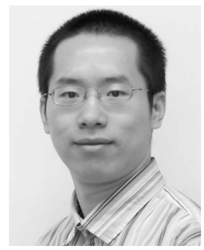

Xuefeng Zeng received the B.S. degree in microelectronic technology from Tianjin University, Tianjin, China, in 2002, the M.S. degree in electronic science and technology from Tsinghua University, Beijing, China, in 2005, and the M.S. and Ph.D. degrees in electrical engineering from the University of Wisconsin, Madison, in 2007 and 2009, respectively.

He is currently a Postdoctoral Research Associate in the Department of Electrical and Computer Engineering, University of Wisconsin, Madison. His research interests include micro/nano fabrication technology and devices, microoptics, microfluidics, biomedical sensors, smart materials, and biomimetics and bioinspiration.

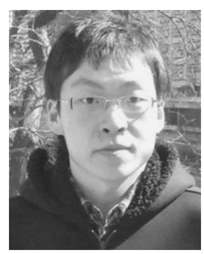

Chenhui Li received the B.S. degree in electrical engineering from Tsinghua University, Beijing, China, in 2007, and the M.S. degree in electrical and computer engineering from the University of Wisconsin, Madison, in 2010. He is currently working toward the Ph.D. degree in electrical engineering at the University of Wisconsin, Madison.

His research interests include microoptical imaging, the liquid focus-variable microlens, electrowetting, and the light field camera.

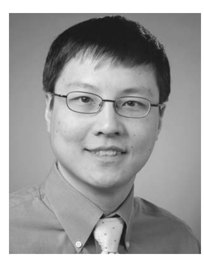

Hongrui Jiang (S’98–M’02–SM’10) received the B.S. degree in physics from Peking University, Beijing, China, and the M.S. and Ph.D. degrees in electrical engineering from Cornell University, Ithaca, NY, in 1999 and 2001, respectively.

He is currently an Associate Professor in the Department of Electrical and Computer Engineering, a Faculty Affiliate in the Department of Biomedical Engineering, a Faculty Member of the Materials Science Program, and a member of the Eye Research Institute, University of Wisconsin, Madison. From 2001 to 2002, he was a Postdoctoral Researcher at the Berkeley Sensor and Actuator Center, University of California, Berkeley. His research interests are in microfabrication technology, biological and chemical microsensors, microactuators, optical microelectromechanical systems, smart materials and micro-/nanostructures, lab-on-a-chip, and biomimetics and bioinspiration.

Dr. Jiang was the recipient of a National Science Foundation CAREER Award and Defense Advanced Research Project Agency Young Faculty Award in 2008, and the H. I. Romnes Faculty Fellowship of the University of Wisconsin, Madison, in 2011.